

Higher Hybrid Bottomonia in an Extended Potential Model

Nosheen Akbar^{*}, M. Atif Sultan[†], Bilal Masud[‡], Faisal Akram[§]

^{*}*COMSATS Institute of Information and Technology, Lahore(54000), Pakistan.*
[†]*Centre For High Energy Physics, University of the Punjab, Lahore(54590), Pakistan.*

Abstract

Using our extension of the quark potential model to hybrid mesons that fits well to the available lattice results, we now calculate the masses, radii, wave functions at origin and E_1 and M_1 radiative transitions for a significant number of bottomonium mesons. These mesons include both conventional and hybrid with radial and angular excitations. Our numerical solutions of the Schrödinger equation are related to QCD through the Born-Oppenheimer approach. Relativistic correction in masses and radiative widths are also calculated by applying leading order perturbation theory. The calculated results are compared with available experimental data and the theoretical results by other groups. We also identify the states of $X_b(10610)$, $Y_b(10890)$, $X(10650)$ and $\chi_b(3P)$ mesons by comparing their experimental masses with our results.

I. Introduction

Models of Quantum chromodynamics (QCD) can be tested by numerical (lattice) simulations of QCD or by hard experiments or, ideally, both. In a series of works [1, 2], we tuned parameters of our extended potential model so that our difference with the available numerical simulations is least and then we test the consequences of our model for (experimentally knowable) meson masses of a variety of J , P (parity) and C states. We provide a comprehensive list of phenomenological implications (masses, radii, wave functions at origin, and E_1 and M_1 radiative transitions for ground and orbitally and radially excited states) that can be obtained through solving the Schrödinger equation for our potential, this time for the new sector of bottomonia. Theoretical interest in this sectors is well known; we can, for example, mention the quotations “The spectroscopy of mesons containing b quarks has been an important testing ground for lattice QCD.” [3] ” and “The $b\bar{b}$ spectroscopy is considered an excellent laboratory to examine the quark-antiquark potential within the non-relativistic framework due to the large b -quark mass.” [4]

We do relativistic corrections and some other refinements to this non-relativistic treatment. Before this, we use Born-Oppenheimer formalism and adiabatic approximation to clarify relationship of our work to QCD. Born-Oppenheimer approach has already been used in hadronic physics in ref. [5] and later in refs. [1, 2, 6]. For relating the angular momenta in our model with experimentally knowable parity P and charge parity C , we use the extension of the quark model provided by the flux tube model [7]. This allows modeling the possible hybrid mesons, with non-trivial gluonic field between quarks, as well. But the flux tube model quark-antiquark potential for hybrids (additional $\frac{\pi}{r}$) was suggested only for large quark antiquark separations

^{*}e mail: nosheenakbar@ciitlahore.edu.pk, noshinakbar@yahoo.com

[†]e mail: atifsultan.chep@pu.edu.pk

[‡]e mail: bilalmasud.chep@pu.edu.pk

[§]e mail: faisal.chep@pu.edu.pk

and we have earlier [1] pointed out that it differs significantly from the results of actual lattice simulations performed. In comparison, the potential model that we suggested has a very good comparison with the lattice results[5]. And being a potential model, it gives masses of ground state hybrid mesons along with those of corresponding orbital and radial excited states. We find these by numerically solving the Schrödinger equation along with our relativistic corrections, and obtain a rather detailed list of properties of conventional and hybrid bottomonium mesons with well specified quantum numbers. Thus a comparison of our calculated meson masses of specified J , P , and C states with experimentally observed masses can help in recognizing the observed mesons like $X_b(10610)$, $Y_b(10890)$, $X(10650)$ and $\chi_b(3P)$.

Heavy hybrid mesons have also been studied using theoretical approaches like constituent gluon model [8, 9, 10], QCD Sum Rule [11, 12, 13, 14, 15, 16, 17, 18], Lattice QCD [6] and Bethe-Salpeter equation [19]. Wherever possible, we compare with their results. Along with calculating masses, in this paper we calculate root mean square radii, radial wave functions at origin, and radiative transitions of the ground and excited states of ordinary and hybrid bottomonium mesons. The results are compared with available experimental and theoretical results. Using the radii one can obtain form factors [20, 21] energy shifts [22, 23], and magnetic polarizabilities [22] for conventional and hybrid bottomonium mesons. Whereas radial wave function at origin can be used in calculating decay rates [24, 25, 24, 26] and differential cross sections [27] of quarkonium states.

The paper is organized as follows. In the section 2, the potential models used for conventional and hybrid mesons are written. Then using these potential models, radial wave functions for the ground and excited states of conventional and hybrid bottomonium mesons are found by numerically solving the Schrödinger equation with relativistic correction subsequently included by perturbation theory. The expressions used to find root mean square radii, radial wave functions at the origin and radiative transitions are also written in this section. Numerical results for these quantities for a variety of conventional and hybrid mesons are reported in section 3. Using our masses for different J^{PC} bottomonium states, we also suggest quantum number assigned to $X_b(10610)$, $Y_b(10890)$, $X(10650)$, and $\chi_b(3P)$. We also report the relevant M_1 and E_1 radiative transitions in this section.

2. Conventional and Hybrid Bottomonium mesons

2.1. Spectrum of conventional mesons

To study the spectrum of conventional bottomonium states we use the following semi-relativistic Hamiltonian carrying lowest order relativistic correction

$$H = 2m_b + \frac{p^2}{2\mu} - \left(\frac{1}{4m_b^3} \right) p^4 + V_{q\bar{q}}(r), \quad (1)$$

where $\mu = m_b/2$ is the reduced mass of the system and m_b is the constituent mass of bottom quark. The effective quark anti-quark potential $V_{q\bar{q}}(r)$ adopted from Ref. [28] carries Gaussian-smeared contact hyperfine interaction, one gluon exchange spin-orbit and tensor terms, and long ranged spin-orbit term in addition to linear plus Coulombic terms. The complete expression of $V_{q\bar{q}}(r)$ is given by

$$\begin{aligned} V_{q\bar{q}}(r) = & \frac{-4\alpha_s}{3r} + br + \frac{32\pi\alpha_s}{9m_b^2} \left(\frac{\sigma}{\sqrt{\pi}} \right)^3 e^{-\sigma^2 r^2} \mathbf{S}_b \cdot \mathbf{S}_{\bar{b}} \\ & + \frac{1}{m_b^2} \left[\left(\frac{2\alpha_s}{r^3} - \frac{b}{2r} \right) \mathbf{L} \cdot \mathbf{S} + \frac{4\alpha_s}{r^3} T \right]. \end{aligned} \quad (2)$$

The Coulombic term which is proportional to strong coupling constant α_s arises from one gluon exchange interaction dominating at short distance, whereas the linear term proportional to string tension b is required to produce confinement in the system. The Gaussian-smeared contact hyperfine interaction proportional to $\mathbf{S}_b \cdot \mathbf{S}_{\bar{b}}$, the short distance spin-orbit, and tensor interactions are also produced by one gluon exchange process, whereas long ranged spin-orbit term is produced by Lorentz scalar confinement. The spin-spin $\mathbf{S}_b \cdot \mathbf{S}_{\bar{b}}$, spin-orbit $\mathbf{L} \cdot \mathbf{S}$, and tensor operators in $|J, L, S\rangle$ basis are given by

$$\mathbf{S}_b \cdot \mathbf{S}_{\bar{b}} = \frac{S(S+1)}{2} - \frac{3}{4} \quad (3a)$$

$$\mathbf{L} \cdot \mathbf{S} = [J(J+1) - L(L+1) - S(S+1)]/2 \quad (3b)$$

$$T = \begin{cases} -\frac{1}{6(2L+3)}, J = L+1 \\ +\frac{1}{6}, J = L \\ -\frac{L+1}{6(2L-1)}, J = L-1. \end{cases} \quad (3c)$$

Here L and S are quantum numbers of the relative orbital angular momentum of quark-antiquark and the total spin angular momentum of the system respectively. Above effective potential carries four unknown parameters strong coupling constant α_s , string tension b , width σ , and bottom quark constituent mass m_b . We fix them by fitting the spectrum to the experimental data of masses of ten well known states of bottomonium mesons given in Table I. The best fit values of these parameters, with relativistic correction, are $\alpha_s = 0.4$, $b = 0.11 \text{ GeV}^2$, $\sigma = 1 \text{ GeV}$, $m_b = 4.89 \text{ GeV}$. In case of non-relativistic Hamiltonian, the best fit parameters are $\alpha_s = 0.36$, $b = 0.1340 \text{ GeV}^2$, $\sigma = 1.34 \text{ GeV}$, $m_b = 4.825 \text{ GeV}$. To calculate the spectrum and the corresponding wave functions of the states of $b\bar{b}$ system we numerically solve the radial Schrödinger equation given by

$$U''(r) + 2\mu(E - V(r) - \frac{\langle L_{q\bar{q}}^2 \rangle}{2\mu r^2})U(r) = 0, \quad (4)$$

where $U(r) = rR(r)$ with $R(r)$ being the radial part of the wave function and $\langle L_{q\bar{q}}^2 \rangle = L(L+1)$. Non-trivial solutions of this equation which exist only for certain discrete values of E are determined by the shooting method. The above Schrödinger equation assumes that the Hamiltonian $H = \frac{p^2}{2\mu} + V_{q\bar{q}}(r)$ i.e., without the constant term $2m_b$ and the relativistic correction. Thus to obtain the mass of a $b\bar{b}$ state we add the constituent quark masses to the energy E which is further corrected by the perturbation theory for the lowest order relativistic correction to the Hamiltonian as given below

$$m_{b\bar{b}} = 2m_b + E + \langle \Psi | \Delta H_{rel} | \Psi \rangle, \quad (5)$$

where $\Delta H_{rel} = -\left(\frac{1}{4m_b^3}\right)p^4$ and Ψ is the complete wave function of $b\bar{b}$ obtained by solving above Schrödinger equation. It is noted that in limit $r \rightarrow 0$ the potential $V_{q\bar{q}}(r) \sim \frac{2\alpha_s}{r^3}(\mathbf{L} \cdot \mathbf{S} + 2T)$. It turns out that corresponding to $S = 1$, $\mathbf{L} \cdot \mathbf{S} + 2T$ is negative for $J = L$ and $J = L - 1$. As a result, the potential becomes strongly attractive at short distance and the resultant wave function becomes unstable in this limit. To circumvent this problem, we calculated the meson masses by solving Schrödinger equation initially without the spin-orbit coupling. The effect of spin-orbit interaction was subsequently included through leading-order perturbative correction to the meson mass. However, calculating the perturbative correction to the wave function is difficult as in this case the contributions comes from all possible mass eigen states. Therefore in this case we applied the smearing of position coordinates, as discussed in Ref. [7], to change the power behaviors of the potential at small distance. In order to show the effect of smearing

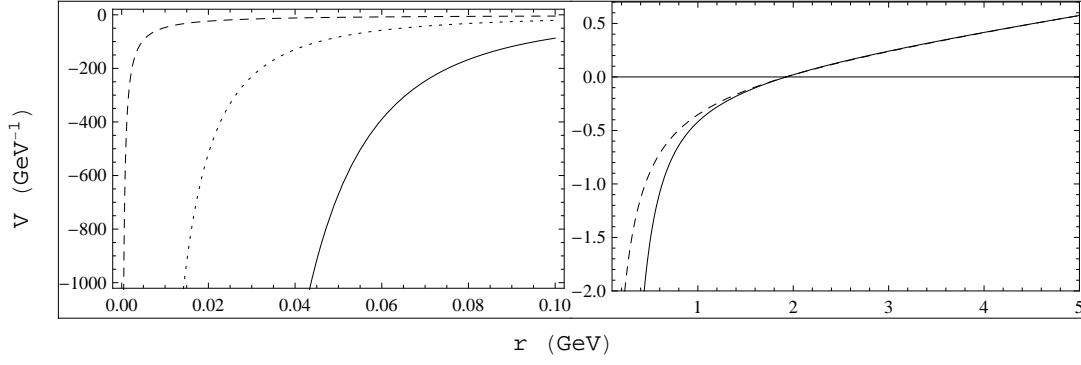


Figure 1: Comparison of potentials with quantum numbers $L = 1$, $S = 1$, and $J = 0$. Solid line represents unsmeared potential without centrifugal term, dotted curve represent the centrifugal term and dashed curve represents the smeared potential. The centrifugal term is inverted for the sake comparison with rest of the terms.

on quark anti-quark effective potential at small distance we give the comparison of smeared and unsmeared potential in Fig. 1. The figure shows that smearing at small distance makes the potential less divergent than $1/r^2$. Thus at small distance repulsive centrifugal potential $l(l+1)/(2\mu r^2)$ would remain dominating even if $\mathbf{L} \cdot \mathbf{S} + 2T$ is negative. The figure also shows that the effect of smearing at large distance is negligible.

2.2.Characteristics of Hybrid Bottomonium mesons

Our study of hybrid meson is based on Born-Oppenheimer (BO) approximation in which energy levels of gluonic field are calculated in the presence of static $q\bar{q}$ pair at fixed distance r by Monte-Carlo estimates of generalized Wilson loops [5]. These energy levels modify the effective $q\bar{q}$ potential $V_{q\bar{q}}(r)$ as following

$$V_{q\bar{q}}^h(r) = V_{q\bar{q}}(r) + V_g(r), \quad (6)$$

where $V_g(r)$ represents the contribution of the gluon field to the effective potential. The functional form of $V_g(r)$ depends on the level of gluonic excitation. In this work we study the hybrid mesons in which gluonic field is in its first excited state and fit the following form of $V_g(r)$

$$V_g(r) = \frac{c}{r} + A \times \exp^{-Br^{0.3723}}. \quad (7)$$

to the available lattice data [5]. We have shown in ref. [1] that this proposed form of $V_g(r)$ provides an excellent fit to the lattice data with best fitted values $A = 3.4693$ GeV, $B = 1.0110$ GeV and $c = 0.1745$. Thus, for the hybrid mesons the radial differential equation is given by

$$U''(r) + 2\mu \left(E - V_{q\bar{q}}^h(r) - \frac{\langle L_{q\bar{q}}^2 \rangle}{2\mu r^2} \right) U(r) = 0, \quad (8)$$

where squared quark anti-quark angular momentum $\langle L_{q\bar{q}}^2 \rangle$ [5, 29] is given by

$$\langle L_{q\bar{q}}^2 \rangle = L(L+1) - 2\Lambda^2 + \langle J_g^2 \rangle. \quad (9)$$

For the first gluonic excitation, the squared gluon angular momentum $\langle J_g^2 \rangle = 2$ and $\Lambda = 1$ [5] making $-2\Lambda^2 + \langle J_g^2 \rangle = 0$.

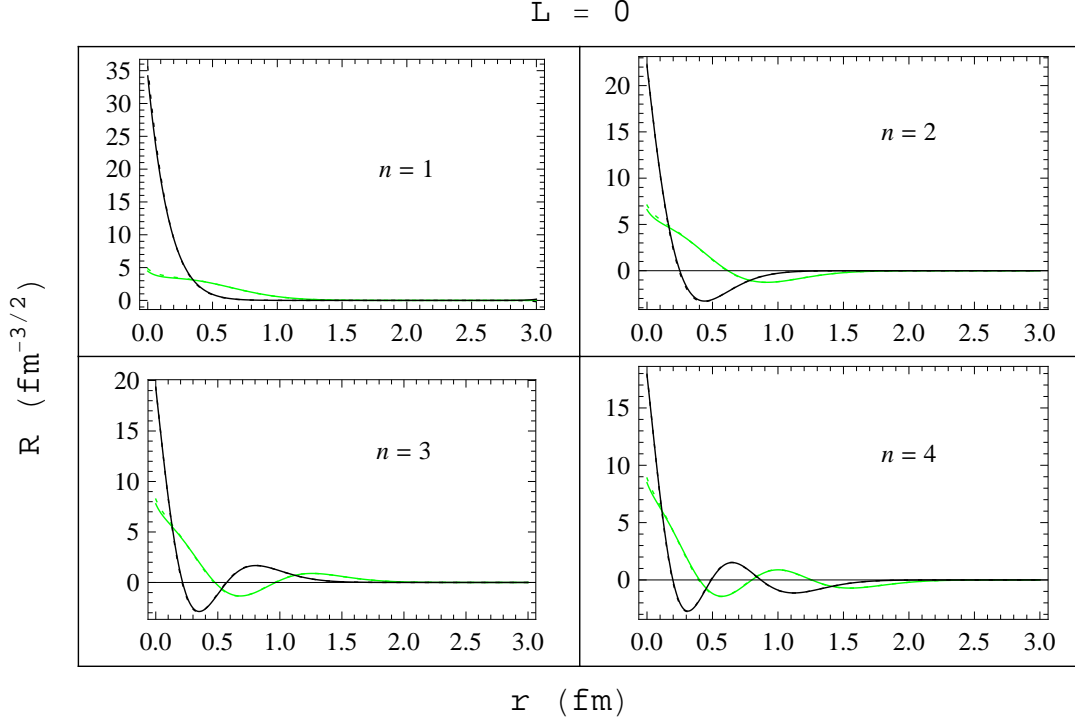


Figure 2: Radial wave functions for radially ground and excited states of η_b and Υ mesons. Black color represents conventional and green color represents hybrid bottomonium mesons. Wave functions of Υ and η_b are almost same within our numerical limits.

Using the hybrid potential of eq. (6), we calculated the masses, radial wave functions of the hybrid mesons by using the same technique as employed for conventional mesons (mentioned above). The effect of relativistic correction is again determined using leading-order perturbation theory. The resultant wave functions are plotted in green color in Figs. 2-5 corresponding to same values of n , L , and S . These figures also show the comparison of the conventional and hybrid meson radial wave functions. The shape of these radial wave functions is not much affected by the addition of the V_g term for hybrids, though the values of masses are significantly increased for the same values of n , L , and S . These normalized wave functions of conventional and hybrid bottomonium mesons are then used to calculate root mean square radii and radial wave functions at origin using the following relations:

$$\sqrt{\langle r^2 \rangle} = \sqrt{\int U^* r^2 U dr}. \quad (10)$$

$$R(0) = U'(0) \text{ for } L = 0. \quad (11)$$

Radial wave functions at origin are found to be zero for $L \geq 1$. The applications of radial wave functions at origin are mentioned above in section 1. Radiative transitions involve the emission of photon and are important for the study of mesons. $E1$ radiative partial widths from meson to meson transitions are calculated by using the following expression mentioned in ref. [28].

$$\Gamma_{E1}(n^{2S+1}L_J \rightarrow n'^{2S'+1}L'_{J'} + \gamma) = \frac{4}{3} C_{fi} \delta_{SS'} e_b^2 \alpha |\langle \Psi_f | r | \Psi_i \rangle|^2 E_\gamma^3 \frac{E_f^{(b\bar{b})}}{M_i^{(b\bar{b})}}. \quad (12)$$

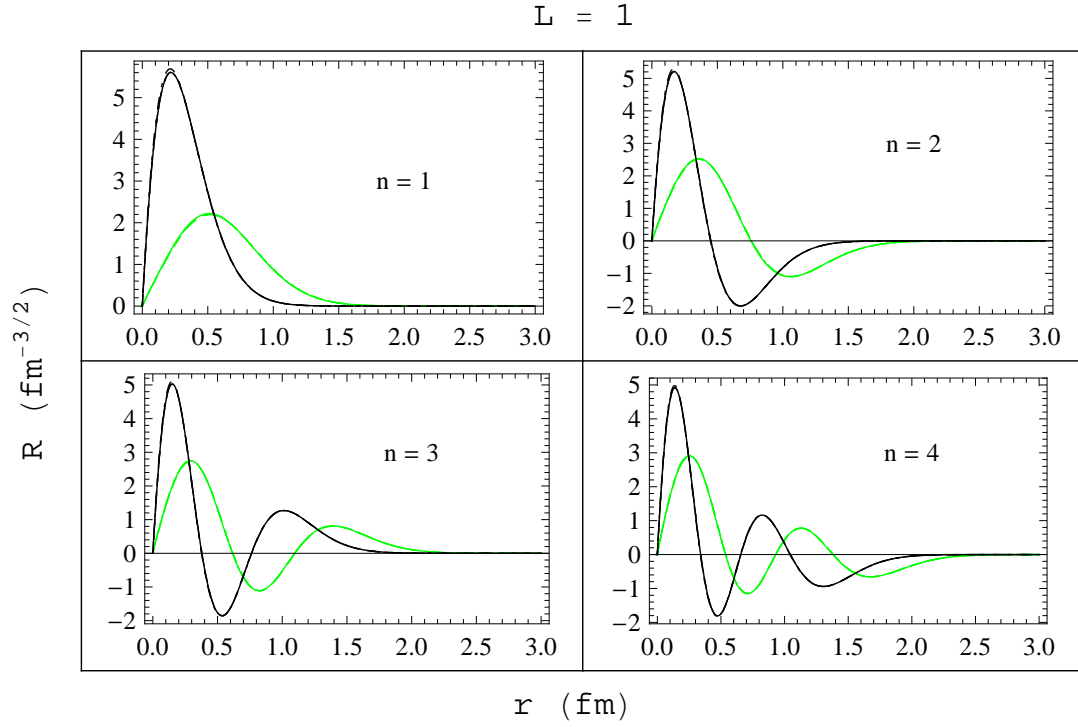


Figure 3: Radial wave functions for radially ground and excited states of χ_{b_0} , χ_{b_1} , χ_{b_2} , and h_b . χ_{b_0} is plotted with solid line, χ_{b_1} with dots, χ_{b_2} with dash, h_b with dot dash. χ_{b_0} , χ_{b_1} , χ_{b_2} , and h_b curves are almost same within our numerical limits. Black color represents conventional and green color represents hybrid bottomonium mesons.

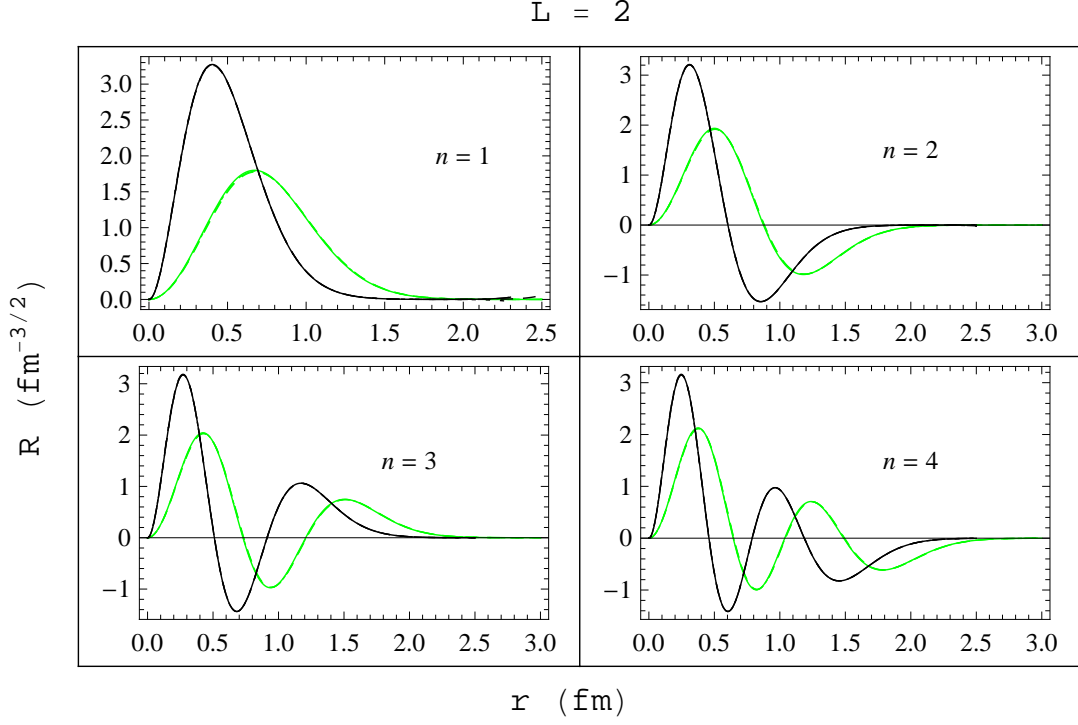


Figure 4: Radial wave functions for radially ground and excited states of $\Upsilon(D)$, Υ_2 , Υ_3 and η_{b2} . Black color represents conventional and green color represents hybrid bottomonium mesons.

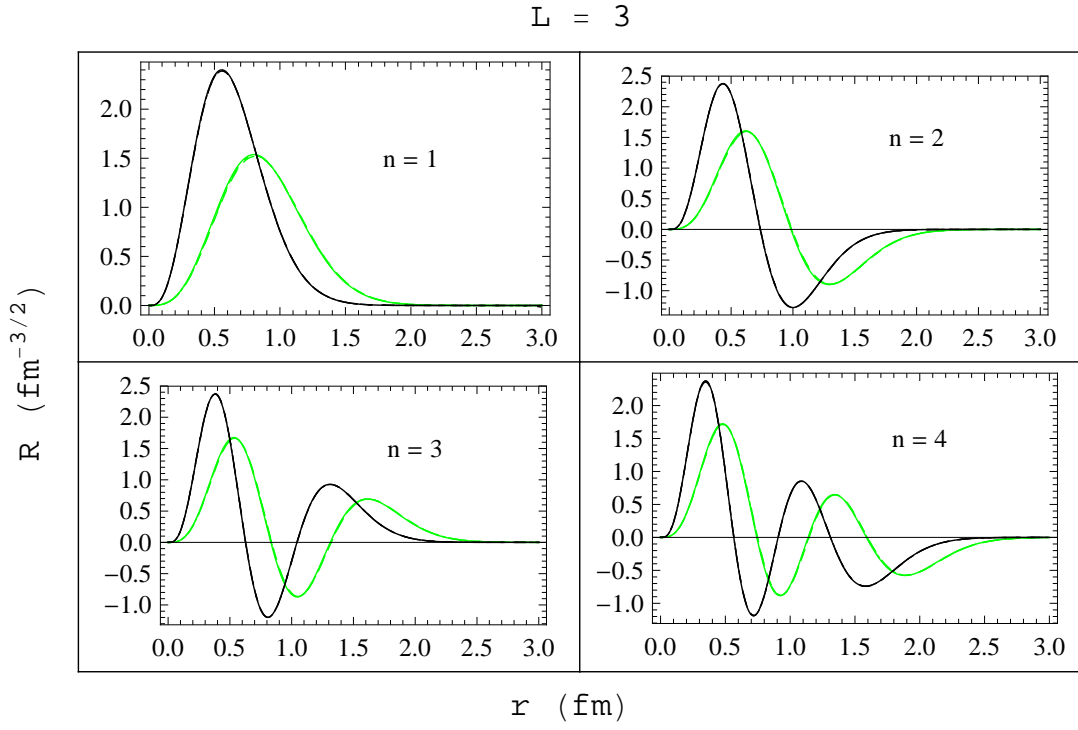


Figure 5: Radial wave functions for radially ground and excited states of χ_2 , χ_3 , χ_4 and h_{b3} are almost same. Black color represents conventional and green color represents hybrid bottomonium mesons.

Here e_b , α , E_γ , $E_f^{b\bar{b}}$, and M_i stand for the bottom quark electric charge in units of charge of electron, electromagnetic fine structure constant, final photon energy, energy of the final $b\bar{b}$ meson, and mass of initial state of bottomonium respectively, and

$$C_{fi} = \max(L, L')(2J' + 1) \left\{ \begin{matrix} L' & J' & S \\ J & L & 1 \end{matrix} \right\}^2. \quad (13)$$

To calculate M_1 radiative partial widths for meson to meson transitions, the following expression [28] is used:

$$\Gamma_{M1}(n^{2S+1}L_J \rightarrow n'^{2S'+1}L'_{J'} + \gamma) = \frac{4}{3} \frac{2J' + 1}{2L + 1} \delta_{LL'} \delta_{SS' \pm 1} e_b^2 \frac{\alpha}{m_b^2} |\langle \Psi_f | \Psi_i \rangle|^2 E_\gamma^3 \frac{E_f^{(b\bar{b})}}{M_i^{(b\bar{b})}}. \quad (14)$$

3. Results and Conclusions

The masses, root mean square radii, radial wave functions at origin, and radiative transitions are calculated for conventional and hybrid bottomonium mesons including the orbital and radial excited J^{PC} states. The calculated masses of bottomonium mesons using the non-relativistic and relativistic Hamiltonian for the ground and excited states are given in Table 1 along with the experimental and theoretical predictions of the other's groups. Table 1 shows that the lowest bottomonium meson's mass is ≈ 9.5 GeV. Masses for hybrid bottomonium mesons using the non-relativistic and relativistic Hamiltonian for the ground state, orbital and radial excited states are reported in Table 2. For differentiating the symbols of conventional and hybrid mesons, a superscript h is used with the corresponding conventional meson symbol having the same values of n , L , and S . This is the same convention used earlier in our ref. [2]. In our calculations, the lowest hybrid bottomonium has $J^{PC} = 0^{++}(0^{--})$ with mass equal to 10.8069 GeV is comparable to results mentioned in ref. [9]. The results given in Table 1 and 2 show that for the same quantum numbers (n , L , and S), the mass of a hybrid meson is significantly greater than the corresponding conventional meson. It is noted that J^{PC} of each hybrid meson is different from the corresponding conventional meson for same L and S . This difference is due to additional quantum numbers (Λ , ε , and η) present in the squared quark anti-quark angular momentum term for hybrid mesons defined in eq.(9) and the following expressions for the parity (P) and charge parity (C) of hybrid mesons.

$$P = \epsilon(-1)^{L+\Lambda+1}, C = \epsilon\eta(-1)^{L+\Lambda+S}, \quad (15)$$

where $\eta = -1$ and $\epsilon = \pm 1$ for Π_u state [5] representing the first gluonic excited state. It is noted that parameter ε has two possible values $+1$ and -1 for first gluonic excited state [5] which we include in the study of hybrid mesons in our present work. As a result we obtain two degenerate hybrid states with opposite values of P and C . For $\varepsilon = 1$ the hybrid mesons are non-exotic, whereas exotic hybrid mesons are obtained for $\varepsilon = -1$ as shown in the Table 2.

By comparing the experimental masses of various X , Y , and Υ particles with our calculated masses having same J^{PC} , some assignments to these experimentally observed particles are suggested as mentioned in Table 3. These results can help in experimentally recognizing hybrid mesons in the bottomonium sector. The comparison of our calculated masses of bottomonium hybrid mesons with others calculated results is given in Table 4. Root mean square radii and radial wave functions at origin for the ground and orbitally and radially excited states of conventional and hybrid bottomonium mesons are reported in Tables 5 and 6 respectively. These

results show that with the same quantum numbers (n , L , and S) root mean square radii of hybrid mesons are greater than conventional mesons. It is also noted that radii of conventional and hybrid mesons increase with radial and angular excitations. Tables 5 and 6 show that $|R(0)|^2$ is non-zero only for S states and decrease with the radial excitation. As scalar form factors [20], energy shifts, and polarizabilities [22] depend on the root mean square radii, we indicate a significant change in the values of these quantities for a hybrid meson as compared to the corresponding conventional meson for the same quantum numbers. Thus it is highly interesting to compare our results with experimental findings of conventional and exotic mesons.

M_1 and E_1 transitions using relativistic and non-relativistic masses are reported in Tables (7-13). Our results for radiative transitions are comparable with experimental and theoretical results of other groups.

Acknowledgement

B. M. and F. A. acknowledge the financial support of Punjab University for the projects (Sr. 215 PU Project 2014-15 and Sr. 220 PU Project 2014-15). N. A. is grateful to Higher education Commission of Pakistan for their financial support (No: PM-IPFP/HRD/HEC/2014/1703).

References

- [1] N. Akbar, B. Masud, S. Noor, Eur. Phys. J. A **47**, 124 (2011); erratum: Eur. Phys. J. A **50**, 121 (2014).
- [2] A. Sultan, N. Akbar, B. Masud, F. Akram, Phys. Rev. D **90**, 054001 (2014).
- [3] A. Gray, I. Allison, C. T. H. Davies, E. Gulez, G. P. Lepage, J. Shigemitsu, M. Wingate, Phys. Rev. D **72**, 094507 (2005).
- [4] T. W. Zhao, C. Lu., Y. Y. Chang, C. Hong, Chinese Physics C **37**, No. 8, 083101 (2013).
- [5] K. J. Juge, J. Kuti, C. J. Morningstar, Nucl. Phys. Proc. Suppl. **63**, 326 (1998).
- [6] E. Braaten, C. Langmack, D. H. Smith, Phys. Rev. D **90**, 014044 (2014).
- [7] N. Isgur, J. Paton, Phys. Rev. D **31**, 2910 (1985).
- [8] F. Iddir, L. Semmla, Int. J. Mod. Phys. A **23**, 5229 (2008).
- [9] F. Iddir, L. Semmla, arXiv:hep-ph/0611165 (2006).
- [10] F. Iddir, L. Semmla, arXiv:hep-ph/0611183 (2006).
- [11] R. Berg, D. Harnett, R. T. Kleiv, T. G. Stee, Phys. Rev. D **86**, 034002 (2012).
- [12] D. Harnett, R. Berg, R. T. Kleiv, T. G. Steele, Nucl. Phys. B Proc. Suppl. **234**, 154 (2013).
- [13] D. Harnett, R. T. Kleiv, T. G. Steele, H. y. Jin, J. Phys. G: Nucl. Part. Phys. **39**, 125003 (2012).
- [14] R. T. Kleiv, D. Harnett, T. G. Steele, H. y. Jin, Nucl. Phys. B. Proc. Suppl. **234**, 150 (2013).
- [15] R. T. Kleiv, B. Bulthuis, D. Harnett, T. Richards, W. Chen, J. Ho, T. G. Steele, Shi-Lin Zhu, Can. J. Phys. **93**, 1 (2015).

Table 1: Masses of ground, radial and orbital excited states of bottomonium meson. Our calculated masses are rounded to 0.0001 GeV.

n	Meson	L	S	J	J^{PC}	Our calculated mass		Theoretical mass with NR potential model	Experimental mass
						Relativistic	NR		
						GeV	GeV	GeV	GeV
1S	$\eta_b(1^1S_0)$	0	0	0	0^{-+}	9.4926	9.5079	9.448 [30], 9.428 [31]	9.4603 ± 0.00026 [32]
	$\Upsilon(1^3S_1)$	0	1	1	1^{--}	9.5098	9.5299	9.459[30], 9.460 [31]	
2 S	$\eta_b(2^1S_0)$	0	0	0	0^{-+}	10.0132	10.0041	10.006[30], 10.190 [31]	10.02326 ± 0.00031 [32]
	$\Upsilon(2^3S_1)$	0	1	1	1^{--}	10.0169	10.0101	10.009[30], 10.219 [31]	
3S	$\eta_b(3^1S_0)$	0	0	0	0^{-+}	10.2792	10.2912	10.352[30], 10.372 [31]	10.3552 ± 0.0005 [32]
	$\Upsilon(3^3S_1)$	0	1	1	1^{--}	10.2815	10.295	10.354[30], 10.401 [31]	
4 S	$\eta_b(4^1S_0)$	0	0	0	0^{-+}	10.4854	10.5214	10.473 [31]	10.5794 ± 0.0012 [32]
	$\Upsilon(4^3S_1)$	0	1	1	1^{--}	10.4872	10.5244	10.502 [31]	
5 S	$\eta_b(5^1S_0)$	0	0	0	0^{-+}	10.6626	10.7226	—	—
	$\Upsilon(5^3S_1)$	0	1	1	1^{--}	10.6642	10.7251	—	
6 S	$\eta_b(6^1S_0)$	0	0	0	0^{-+}	10.8219	10.9053	—	—
	$\Upsilon(6^3S_1)$	0	1	1	1^{--}	10.8233	11.9074	—	
1P	$h_b(1^1P_1)$	1	0	1	1^{+-}	9.9672	9.9279	9.871[30], 10.1160 [31] 9.897[30], 10.190 [31] 9.916[30], 10.219 [31]	9.8993 ± 0.0001 [32]
	$\chi_0(1^3P_0)$	1	1	0	0^{++}	9.8510	9.9232		$9.85944 \pm 0.00042 \pm 0.00031$ [32]
	$\chi_1(1^3P_1)$	1	1	1	1^{++}	9.9612	9.9295		$9.89278 \pm 0.00026 \pm 0.00031$ [32]
	$\chi_2(1^3P_2)$	1	1	2	2^{++}	9.9826	9.9326		$9.91221 \pm 0.00026 \pm 0.00031$ [32]
2 P	$h_b(2^1P_1)$	1	0	1	1^{+-}	10.2342	10.2213	10.232[30], 10.343 [31] 10.255[30], 10.372 [31] 10.271[30], 10.401 [31]	—
	$\chi_0(2^3P_0)$	1	1	0	0^{++}	10.2098	10.2197		$10.2325 \pm 0.0004 \pm 0.0005$ [32]
	$\chi_1(2^3P_1)$	1	1	1	1^{++}	10.2306	10.2232		$10.25546 \pm 0.00022 \pm 0.00050$ [32]
	$\chi_2(2^3P_2)$	1	1	2	2^{++}	10.2447	10.2245		$10.26865 \pm 0.00022 \pm 0.00050$ [32]
3 P	$h_b(3^1P_1)$	1	0	1	1^{+-}	10.4423	10.456	10.444 [31]	—
	$\chi_0(3^3P_0)$	1	1	0	0^{++}	10.4239	10.4557	10.522[30], 10.473 [31]	—
	$\chi_1(3^3P_1)$	1	1	1	1^{++}	10.4396	10.4579	10.544[30], 10.502 [31]	—
	$\chi_2(3^3P_2)$	1	1	2	2^{++}	10.4507	10.4585	10.559[30]	—
4 P	$h_b(4^1P_1)$	1	0	1	1^{+-}	10.6213	10.6606	10.521 [31]	—
	$\chi_0(4^3P_0)$	1	1	0	0^{++}	10.606	10.6607	10.550 [31]	—
	$\chi_1(4^3P_1)$	1	1	1	1^{++}	10.619	10.6624	10.579 [31]	—
	$\chi_2(4^3P_2)$	1	1	2	2^{++}	10.6284	10.6627	—	—
5 P	$h_b(5^1P_1)$	1	0	1	1^{+-}	10.7822	10.8459	—	—
	$\chi_0(5^3P_0)$	1	1	0	0^{++}	10.7688	10.8463	—	—
	$\chi_1(5^3P_1)$	1	1	1	1^{++}	10.7802	10.8476	—	—
	$\chi_2(5^3P_2)$	1	1	2	2^{++}	10.7884	10.8478	—	—
6 P	$h_b(6^1P_1)$	1	0	1	1^{+-}	10.9302	11.0176	—	—
	$\chi_0(6^3P_0)$	1	1	0	0^{++}	10.9182	11.0181	—	—
	$\chi_1(6^3P_1)$	1	1	1	1^{++}	10.9284	11.0192	—	—
	$\chi_2(6^3P_2)$	1	1	2	2^{++}	10.9358	11.0192	—	—
1 D	$\eta_{b2}(1^1D_2)$	2	0	2	2^{-+}	10.1661	10.1355	10.155 [6]	—
	$\Upsilon(1^3D_1)$	2	1	1	1^{--}	10.1548	10.1299		10.1637 ± 0.00014 [32]
	$\Upsilon_2(1^3D_2)$	2	1	2	2^{--}	10.1649	10.1351		
	$\Upsilon_3(1^3D_3)$	2	1	3	3^{--}	10.1772	10.1389		—

n	Meson	L	S	J	J^{PC}	Our calculated mass	
						Relativistic	NR
						GeV	GeV
2 D	$\eta_{b2}(2^1 D_2)$	2	0	2	2^{-+}	10.3801	10.3779
	$\Upsilon(2^3 D_1)$	2	1	1	1^{--}	10.3688	10.3751
	$\Upsilon_2(2^3 D_2)$	2	1	2	2^{--}	10.3789	10.378
	$\Upsilon_3(2^3 D_3)$	2	1	3	3^{--}	10.3864	10.3799
3 D	$\eta_{b2}(3^1 D_2)$	2	0	2	2^{-+}	10.5633	10.5877
	$\Upsilon(3^3 D_1)$	2	1	1	1^{--}	10.5525	10.5861
	$\Upsilon_2(3^3 D_2)$	2	1	2	2^{--}	10.5621	10.5881
	$\Upsilon_3(3^3 D_3)$	2	1	3	3^{--}	10.5695	10.5892
4 D	$\eta_{b2}(4^1 D_2)$	2	0	2	2^{-+}	10.7273	10.777
	$\Upsilon(4^3 D_1)$	2	1	1	1^{--}	10.717	10.776
	$\Upsilon_2(4^3 D_2)$	2	1	2	2^{--}	10.7262	10.7775
	$\Upsilon_3(4^3 D_3)$	2	1	3	3^{--}	10.7334	10.7782
5 D	$\eta_{b2}(5^1 D_2)$	2	0	2	2^{-+}	10.8779	10.9518
	$\Upsilon(5^3 D_1)$	2	1	1	1^{--}	10.8681	10.9512
	$\Upsilon_2(5^3 D_2)$	2	1	2	2^{--}	10.8768	10.9524
	$\Upsilon_3(5^3 D_3)$	2	1	3	3^{--}	10.8839	10.9528
1 F	$h_{b3}(1^1 F_3)$	3	0	3	3^{+-}	10.3116	10.2941
	$\chi_2(1^3 F_2)$	3	1	2	2^{++}	10.308	10.2894
	$\chi_3(1^3 F_3)$	3	1	3	3^{++}	10.3114	10.2937
	$\chi_4(1^3 F_4)$	3	1	4	4^{++}	10.3137	10.297
2 F	$h_{b3}(2^1 F_3)$	3	0	3	3^{+-}	10.5	10.5102
	$\chi_2(2^3 F_2)$	3	1	2	2^{++}	10.4956	10.5074
	$\chi_3(2^3 F_3)$	3	1	3	3^{++}	10.4997	10.5101
	$\chi_4(2^3 F_4)$	3	1	4	4^{++}	10.5027	10.5119
3 F	$h_{b3}(3^1 F_3)$	3	0	3	3^{+-}	10.6679	10.7041
	$\chi_2(3^3 F_2)$	3	1	2	2^{++}	10.6629	10.7022
	$\chi_3(3^3 F_3)$	3	1	3	3^{++}	10.6676	10.7041
	$\chi_4(3^3 F_4)$	3	1	4	4^{++}	10.6711	10.7053
4 F	$h_{b3}(4^1 F_3)$	3	0	3	3^{+-}	10.8216	10.8825
	$\chi_2(4^3 F_2)$	3	1	2	2^{++}	10.8162	10.8811
	$\chi_3(4^3 F_3)$	3	1	3	3^{++}	10.8212	10.8826
	$\chi_4(4^3 F_4)$	3	1	4	4^{++}	10.825	10.8835

Table 2: Our calculated masses of $b\bar{b}$ hybrid bottomonium mesons.

n	Meson	L	S	J	J^{PC}		Our calculated mass	
					$\varepsilon = 1$	$\varepsilon = -1$	Relativistic	NR
							GeV	GeV
1S	$\eta_b^h(1^1S_0)$	0	0	0	0^{++}	0^{--}	10.8069	10.7734
	$\Upsilon^h(1^3S_1)$	0	1	1	1^{+-}	1^{-+}	10.8079	10.7747
2S	$\eta_b^h(2^1S_0)$	0	0	0	0^{++}	0^{--}	10.9262	10.9187
	$\Upsilon^h(2^3S_1)$	0	1	1	1^{+-}	1^{-+}	10.928	10.9211
3S	$\eta_b^h(3^1S_0)$	0	0	0	0^{++}	0^{--}	11.0459	11.0636
	$\Upsilon^h(3^3S_1)$	0	1	1	1^{+-}	1^{-+}	11.048	11.0664
4S	$\eta_b^h(4^1S_0)$	0	0	0	0^{++}	0^{--}	11.1642	11.2057
	$\Upsilon^h(4^3S_1)$	0	1	1	1^{+-}	1^{-+}	11.1662	11.2086
5S	$\eta_b^h(5^1S_0)$	0	0	0	0^{++}	0^{--}	11.2798	11.3442
	$\Upsilon^h(5^3S_1)$	0	1	1	1^{+-}	1^{-+}	11.2817	11.3469
6S	$\eta_b^h(6^1S_0)$	0	0	0	0^{++}	0^{--}	11.3924	11.4789
	$\Upsilon^h(6^3S_1)$	0	1	1	1^{+-}	1^{-+}	11.394	11.4814
1P	$h_b^h(1^1P_1)$	1	0	1	1^{--}	1^{++}	10.8561	10.8357
	$\chi_0^h(1^3P_0)$	1	1	0	0^{-+}	0^{+-}	10.8534	10.8325
	$\chi_1^h(1^3P_1)$	1	1	1	1^{-+}	1^{+-}	10.8559	10.8354
	$\chi_2^h(1^3P_2)$	1	1	2	2^{-+}	2^{+-}	10.8569	10.8366
2P	$h_b^h(2^1P_1)$	1	0	1	1^{--}	1^{++}	10.984	10.9889
	$\chi_0^h(2^3P_0)$	1	1	0	0^{-+}	0^{+-}	10.9792	10.9868
	$\chi_1^h(2^3P_1)$	1	1	1	1^{-+}	1^{+-}	10.9835	10.989
	$\chi_2^h(2^3P_2)$	1	1	2	2^{-+}	2^{+-}	10.9856	10.9897
3P	$h_b^h(3^1P_1)$	1	0	1	1^{--}	1^{++}	11.1074	11.1363
	$\chi_0^h(3^3P_0)$	1	1	0	0^{-+}	0^{+-}	11.1012	11.135
	$\chi_1^h(3^3P_1)$	1	1	1	1^{-+}	1^{+-}	11.1066	11.1367
	$\chi_2^h(3^3P_2)$	1	1	2	2^{-+}	2^{+-}	11.1097	11.1372
4P	$h_b^h(4^1P_1)$	1	0	1	1^{--}	1^{++}	11.2266	11.2786
	$\chi_0^h(4^3P_0)$	1	1	0	0^{-+}	0^{+-}	11.2195	11.2777
	$\chi_1^h(4^3P_1)$	1	1	1	1^{-+}	1^{+-}	11.2257	11.2791
	$\chi_2^h(4^3P_2)$	1	1	2	2^{-+}	2^{+-}	11.2293	11.2795
5P	$h_b^h(5^1P_1)$	1	0	1	1^{--}	1^{++}	11.3418	11.4161
	$\chi_0^h(5^3P_0)$	1	1	0	0^{-+}	0^{+-}	11.3342	11.4155
	$\chi_1^h(5^3P_1)$	1	1	1	1^{-+}	1^{+-}	11.3408	11.4167
	$\chi_2^h(5^3P_2)$	1	1	2	2^{-+}	2^{+-}	11.3448	11.417
6P	$h_b^h(6^1P_1)$	1	0	1	1^{--}	1^{++}	11.4534	11.5493
	$\chi_0^h(6^3P_0)$	1	1	0	0^{-+}	0^{+-}	11.4456	11.549
	$\chi_1^h(6^3P_1)$	1	1	1	1^{-+}	1^{+-}	11.4524	11.5501
	$\chi_2^h(6^3P_2)$	1	1	2	2^{-+}	2^{+-}	11.4566	11.5503
1D	$\eta_{b2}(1^1D_2)$	2	0	2	2^{++}	2^{--}	10.9125	10.9053
	$\Upsilon^h(1^3D_1)$	2	1	1	1^{+-}	1^{-+}	10.9119	10.9032
	$\Upsilon_2^h(1^3D_2)$	2	1	2	2^{+-}	2^{-+}	10.9126	10.9052
	$\Upsilon_3^h(1^3D_3)$	2	1	3	3^{+-}	3^{-+}	10.9127	10.9063
2D	$\eta_{b2}^h(2^1D_2)$	2	0	2	2^{++}	2^{--}	11.0409	11.0583
	$\Upsilon^h(2^3D_1)$	2	1	1	1^{+-}	1^{-+}	11.0395	11.0566
	$\Upsilon_2^h(2^3D_2)$	2	1	2	2^{+-}	2^{-+}	11.0408	11.0582
	$\Upsilon_3^h(2^3D_3)$	2	1	3	3^{+-}	3^{-+}	11.0415	11.0591

n	Meson	L	S	J	J^{PC}		Our calculated mass	
					$\varepsilon = 1$	$\varepsilon = -1$	Relativistic	NR
							GeV	GeV
3 D	$\eta_{b2}^h(3^1D_2)$	2	0	2	2^{++}	2^{--}	11.1639	11.2047
	$\Upsilon^h(3^3D_1)$	2	1	1	1^{+-}	1^{-+}	11.1618	11.2034
	$\Upsilon_2^h(3^3D_2)$	2	1	2	2^{+-}	2^{-+}	11.1638	11.2048
	$\Upsilon_3^h(3^3D_3)$	2	1	3	3^{+-}	3^{-+}	11.165	11.2054
4 D	$\eta_{b2}^h(4^1D_2)$	2	0	2	2^{++}	2^{--}	11.2823	11.3457
	$\Upsilon^h(4^3D_1)$	2	1	1	1^{+-}	1^{-+}	11.2796	11.3446
	$\Upsilon_2^h(4^3D_2)$	2	1	2	2^{+-}	2^{-+}	11.2821	11.3458
	$\Upsilon_3^h(4^3D_3)$	2	1	3	3^{+-}	3^{-+}	11.2837	11.3463
5 D	$\eta_{b2}^h(1^1D_2)$	2	0	2	2^{++}	2^{--}	11.3965	11.4818
	$\Upsilon^h(5^3D_1)$	2	1	1	1^{+-}	1^{-+}	11.3933	11.4809
	$\Upsilon_2^h(5^3D_2)$	2	1	2	2^{+-}	2^{-+}	11.3962	11.4819
	$\Upsilon_3^h(5^3D_3)$	2	1	3	3^{+-}	3^{-+}	11.3983	11.4823
1 F	$h_{b3}^h(1^1F_3)$	3	0	3	3^{--}	3^{++}	10.9727	10.9787
	$\chi_2^h(1^3F_2)$	3	1	2	2^{-+}	2^{+-}	10.9729	10.9774
	$\chi_3^h(1^3F_3)$	3	1	3	3^{-+}	3^{+-}	10.9729	10.9787
	$\chi_4^h(1^3F_4)$	3	1	4	4^{-+}	4^{+-}	10.9724	10.9793
2 F	$h_{b3}^h(2^1F_3)$	3	0	3	3^{--}	3^{++}	11.0995	11.1293
	$\chi_2^h(2^3F_2)$	3	1	2	2^{-+}	2^{+-}	11.0993	11.1281
	$\chi_3^h(2^3F_3)$	3	1	3	3^{-+}	3^{+-}	11.0996	11.1293
	$\chi_4^h(2^3F_4)$	3	1	4	4^{-+}	4^{+-}	11.0995	11.13
3 F	$h_{b3}^h(3^1F_3)$	3	0	3	3^{--}	3^{++}	11.221	11.2736
	$\chi_2^h(3^3F_2)$	3	1	2	2^{-+}	2^{+-}	11.2204	11.2725
	$\chi_3^h(3^3F_3)$	3	1	3	3^{-+}	3^{+-}	11.221	11.2737
	$\chi_4^h(3^3F_4)$	3	1	4	4^{-+}	4^{+-}	11.2212	11.2742
4 F	$h_{b3}^h(4^1F_3)$	3	0	3	3^{--}	3^{++}	11.3378	11.4126
	$\chi_2^h(4^3F_2)$	3	1	2	2^{-+}	2^{+-}	11.3369	11.4116
	$\chi_3^h(4^3F_3)$	3	1	3	3^{-+}	3^{+-}	11.3378	11.4126
	$\chi_4^h(4^3F_4)$	3	1	4	4^{-+}	4^{+-}	11.3383	11.4131

Table 3: Our assignments based on the equivalence of calculated and experimentally measured values of masses and J^{PC} .

Meson	J^{PC}	Experimental mass	Assignments
		GeV	
$\chi_b(3P)$	$?^{?+}$	10.534 ± 0.009 [32]	$\chi_{b0}(3^3P_0), \chi_{b1}(3^3P_1), \chi_{b2}(3^3P_2)$
$\Upsilon(10860)$	1^{--}	10.876 ± 0.011 [32]	$\Upsilon(6^3S_1), h_b^h(1^1P_1)$
$\Upsilon(11020)$	1^{--}	11.019 ± 0.008 [32]	$h_b^h(2^1P_1), h_b^h(3^1P_1)$
$X(10650)$	$1^{+?}$	10.6522 ± 0.015 [32]	$h_b(4^1P_1), \chi_1(4^3P_1)$
$Y_b(10890)$	1^{+-}		$h_b(5^1P_1), h_b^h(6^1P_1), \Upsilon^h(1^3S_1)$
$X_b(10610)$	$1^{+?}$	10.607 ± 0.002 [32]	$h_b(4^1P_1), \chi_1(4^3P_1)$

Table 4: Masses (in GeV) of hybrid bottomonium mesons calculated by other models along with our calculated results. Our results are reported for J^{PC} states with lowest orbital angular momentum (L).

J^{PC} state	Our results		NRLQCD		LQCD [6]	QCD Sum Rule [18][34]	Potential Model [9]	Quark model and QCDME [33]
	Ground state	First radial excited state	Ground state [6]	First radial [6]				
0^{--}	10.8069	10.9262	-		-	11.48 ± 0.75	11.02	
1^{--}	10.8561	10.984	10.559	10.977+0.041		9.7 ± 0.12	11.12	10.785
0^{-+}	10.8534	10.9792				9.68 ± 0.29	10.96	
1^{-+}	10.8079	10.928			10.559	9.79 ± 0.22	10.98	
1^{+-}	10.8079	10.928				10.70 ± 0.53		
0^{+-}	10.8534	10.9792		-	10.159 ± 0.362	10.17 ± 0.22	10.86	
1^{++}	10.8561	10.984	10.597 ± 0.065	-	-	11.09 ± 0.60	-	
0^{++}	10.8069	10.9262	10.892 ± 0.036	-	-	11.20 ± 0.48	-	
2^{+-}	10.8569	10.9856	-	-	11.323 ± 0.257	-	-	
2^{-+}	10.8569	10.9856	-	-		9.93 ± 0.21	-	
2^{++}	10.9125	11.0409	-	-		10.64 ± 0.33	-	

- [16] W. Chen, J. Ho, T. G. Steele, R. T. Kleiv, B. Bulthuis, D. Harnett, T. Richards, Shi-Lin Zhu, Proceedings, 30th International Workshop on High Energy Physics: Particle and Astroparticle Physics, Gravitation and Cosmology: Predictions, Observations and New Projects (IHEP 2014) : Protvino, Russia, June 23-27, (2014).
- [17] C. F. Qiaoa, L. Tang, G. Hao, Xue-Qian Li, J. Phys. G **39**, 015005 (2012).
- [18] W. Chen, T. G. Steele, Shi-Lin Zhu, THE UNIVERSE, **2**, 1 (2014).
- [19] J. Y. Cui, H. Y. Jin, J. M. Wu , Int. J. Mod. Phys. A **14**, 2273 (1999).
- [20] B. Ananthanarayan, I. Caprini, G. Colangelo, J. Gasser and H. Leutwyler, Phys. Lett. B **602**, 218 (2004).
- [21] Kevin L. Haglin, proceedings of the 18th Winter Workshop on Nuclear Dynamics, Nassau, Bahamas, January 20-27 (2002).
- [22] S. I. Kruglov, Phys. Rev. D **60**, 116009 (1999).
- [23] Hai-bin Wang, York-Peng Yao, Phys. Rev. D **70**, 094046 (2004).
- [24] B. Patel and P. C. Vinodkumar, J. Phys. G **36**, 035003 (2009) and reference there in.
- [25] Hong-Wei Ke, Xue-Qian Li, Zheng-Tao Wei, Xiang Liu, Phys. Rev. D **82**, 034023 (2010).
- [26] Estia J. Eichten, Chris Quigg, Phys. Rev. D **52**, 1726 (1995).
- [27] C. H. Chaug, C. F. Qiao, J. X. Wang, Phys. Rev. D **57**, 4035 (1998).
- [28] T. Barnes, S. Godfrey, and E. S. Swanson, Phys. Rev. D **72**, 054026 (2005).
- [29] K. J. Juge, J. Kuti, and C. J. Morningstar, Phys. Rev. Lett., **82**, 4400 (1999).
- [30] O. Lakhina, E. S. Swanson, phys Rev D **74**, 014012, (2006).
- [31] Tanja Branz, Thomas Gutsche, Valery E. Lyubovitskij, Ivan Schmidt, Alfredo Vega, Phys. Rev. D **82**, 074022 (2010).

Table 5: Root mean square radii and square of radial wave function at origin for ground state and orbital and radial excited states of bottomonium meson.

n	Meson	L	S	J	J^{PC}	our calculated $\sqrt{\langle r^2 \rangle}$	Theor. $\sqrt{\langle r^2 \rangle}$ with potential model [35]	Our calculated $ R(0) ^2$
						fm	fm	GeV^3
1S	$\eta_b(1^1S_0)$	0	0	0	0^{-+}	0.2265	-	9.6945
	$\Upsilon(1^3S_1)$	0	1	1	1^{--}	0.2328	0.23	8.9763
2 S	$\eta_b(2^1S_0)$	0	0	0	0^{-+}	0.5408	-	3.8115
	$\Upsilon(2^3S_1)$	0	1	1	1^{--}	0.5448	0.52	3.7568
3S	$\eta_b(3^1S_0)$	0	0	0	0^{-+}	0.8018	-	2.8709
	$\Upsilon(3^3S_1)$	0	1	1	1^{--}	0.8047	0.78	2.8464
4 S	$\eta_b(4^1S_0)$	0	0	0	0^{-+}	1.0273	-	2.4689
	$\Upsilon(4^3S_1)$	0	1	1	1^{--}	1.0296	1.02	2.4517
5 S	$\eta_b(5^1S_0)$	0	0	0	0^{-+}	-	-	2.236
	$\Upsilon(5^3S_1)$	0	1	1	1^{--}	1.2324	1.24	2.222
6 S	$\eta_b(6^1S_0)$	0	0	0	0^{-+}	-	-	2.0799
	$\Upsilon(6^3S_1)$	0	1	1	1^{--}	1.4195	1.45	2.0675
1P	$h_b(1^1P_1)$	1	0	1	1^{+-}	0.4347	-	≈ 0
	$\chi_0(1^3P_0)$	1	1	0	0^{++}	0.4375	-	≈ 0
	$\chi_1(1^3P_1)$	1	1	1	1^{++}	0.4379	-	≈ 0
	$\chi_2(1^3P_2)$	1	1	2	2^{++}	0.4375	0.42	≈ 0
2 P	$h_b(2^1P_1)$	1	0	1	1^{+-}	0.7114	-	≈ 0
	$\chi_0(2^3P_0)$	1	1	0	0^{++}	0.7132	-	≈ 0
	$\chi_1(2^3P_1)$	1	1	1	1^{++}	0.7139	-	≈ 0
	$\chi_2(2^3P_2)$	1	1	2	2^{++}	0.7139	0.69	≈ 0
3 P	$h_b(3^1P_1)$	1	0	1	1^{+-}	0.9453	-	≈ 0
	$\chi_0(3^3P_0)$	1	1	0	0^{++}	0.9470	-	≈ 0
	$\chi_1(3^3P_1)$	1	1	1	1^{++}	0.9476	-	≈ 0
	$\chi_2(3^3P_2)$	1	1	2	2^{++}	0.9474	0.93	≈ 0
4 P	$h_b(4^1P_1)$	1	0	1	1^{+-}	1.1541	-	≈ 0
	$\chi_0(4^3P_0)$	1	1	0	0^{++}	1.1557	-	≈ 0
	$\chi_1(4^3P_1)$	1	1	1	1^{++}	1.1561	-	≈ 0
	$\chi_2(4^3P_2)$	1	1	2	2^{++}	1.1559	1.15	≈ 0
5 P	$h_b(5^1P_1)$	1	0	1	1^{+-}	1.3457	-	≈ 0
	$\chi_0(5^3P_0)$	1	1	0	0^{++}	1.3472	-	≈ 0
	$\chi_1(5^3P_1)$	1	1	1	1^{++}	1.3475	-	≈ 0
	$\chi_2(5^3P_2)$	1	1	2	2^{++}	1.3473	1.37	≈ 0
6 P	$h_b(6^1P_1)$	1	0	1	1^{+-}	1.5246	-	≈ 0
	$\chi_0(6^3P_0)$	1	1	0	0^{++}	1.5261	-	≈ 0
	$\chi_1(6^3P_1)$	1	1	1	1^{++}	1.5263	-	≈ 0
	$\chi_2(6^3P_2)$	1	1	2	2^{++}	1.5260	-	≈ 0
1 D	$\eta_{b2}(1^1D_2)$	2	0	2	2^{-+}	0.5933	-	≈ 0
	$\Upsilon(1^3D_1)$	2	1	1	1^{--}	0.5930	-	≈ 0
	$\Upsilon_2(1^3D_2)$	2	1	2	2^{--}	0.5939	0.6	≈ 0
	$\Upsilon_3(1^3D_3)$	2	1	3	3^{--}	0.5942	0.57	≈ 0

n	Meson	L	S	J	J^{PC}	our calculated $\sqrt{\langle r^2 \rangle}$ [35]	Others calculated $\sqrt{\langle r^2 \rangle}$	$ R(0) ^2$
						fm	fm	GeV^3
2 D	$\eta_{b2}(2^1D_2)$	2	0	2	2^{-+}	0.8447	-	≈ 0
	$\Upsilon(2^3D_1)$	2	1	1	1^{--}	0.8448		≈ 0
	$\Upsilon_2(2^3D_2)$	2	1	2	2^{--}	0.8455		≈ 0
	$\Upsilon_3(2^3D_3)$	2	1	3	3^{--}	0.8457		≈ 0
3 D	$\eta_{b2}(3^1D_2)$	2	0	2	2^{-+}	1.0634	1.05	≈ 0
	$\Upsilon(3^3D_1)$	2	1	1	1^{--}	1.0638		≈ 0
	$\Upsilon_2(3^3D_2)$	2	1	2	2^{--}	1.0643		≈ 0
	$\Upsilon_3(3^3D_3)$	2	1	3	3^{--}	1.0643		≈ 0
4 D	$\eta_{b2}(4^1D_2)$	2	0	2	2^{-+}	1.2616	1.27	≈ 0
	$\Upsilon(4^3D_1)$	2	1	1	1^{--}	1.2623		≈ 0
	$\Upsilon_2(4^3D_2)$	2	1	2	2^{--}	1.2626		≈ 0
	$\Upsilon_3(4^3D_3)$	2	1	3	3^{--}	1.2625		≈ 0
5 D	$\eta_{b2}(5^1D_2)$	2	0	2	2^{-+}	1.4455	1.49	≈ 0
	$\Upsilon(5^3D_1)$	2	1	1	1^{--}	1.4463		≈ 0
	$\Upsilon_2(5^3D_2)$	2	1	2	2^{--}	1.4465		≈ 0
	$\Upsilon_3(5^3D_3)$	2	1	3	3^{--}	1.4463		≈ 0
1 F	$h_{b3}(1^1F_3)$	3	0	3	3^{+-}	0.7280		≈ 0
	$\chi_2(1^3F_2)$	3	1	2	2^{++}	0.7266		≈ 0
	$\chi_3(1^3F_3)$	3	1	3	3^{++}	0.728		≈ 0
	$\chi_4(1^3F_4)$	3	1	4	4^{++}	0.7289		≈ 0
2 F	$h_{b3}(2^1F_3)$	3	0	3	3^{+-}	0.9619		≈ 0
	$\chi_2(2^3F_2)$	3	1	2	2^{++}	0.9611		≈ 0
	$\chi_3(2^3F_3)$	3	1	3	3^{++}	0.9619		≈ 0
	$\chi_4(2^3F_4)$	3	1	4	4^{++}	0.9623		≈ 0
3 F	$h_{b3}(3^1F_3)$	3	0	3	3^{+-}	1.1688		≈ 0
	$\chi_2(3^3F_2)$	3	1	2	2^{++}	1.1696		≈ 0
	$\chi_3(3^3F_3)$	3	1	3	3^{++}	1.1701		≈ 0
	$\chi_4(3^3F_4)$	3	1	4	4^{++}	1.1702		≈ 0
4 F	$h_{b3}(4^1F_3)$	3	0	3	3^{+-}	1.3621		≈ 0
	$\chi_2(4^3F_2)$	3	1	2	2^{++}	1.3563		≈ 0
	$\chi_3(4^3F_3)$	3	1	3	3^{++}	1.3567		≈ 0
	$\chi_4(4^3F_4)$	3	1	4	4^{++}	1.3564		≈ 0

Table 6: Our calculated root mean square radii and $|R(0)|^2$ of $b\bar{b}$ hybrid mesons.

n	Meson	L	S	J	J^{PC}		our calculated $\sqrt{\langle r^2 \rangle}$	Our calculated $ R(0) ^2$
					$\varepsilon = 1$	$\varepsilon = -1$		
							fm	GeV^3
1S	$\eta_b^h(1^1S_0)$	0	0	0	0^{++}	0^{--}	0.6215	0.1795
	$\Upsilon^h(1^3S_1)$	0	1	1	1^{+-}	1^{-+}	0.6272	0.1530
2 S	$\eta_b^h(2^1S_0)$	0	0	0	0^{++}	0^{--}	0.874	0.3856
	$\Upsilon^h(2^3S_1)$	0	1	1	1^{+-}	1^{-+}	0.8801	0.3343
3S	$\eta_b^h(3^1S_0)$	0	0	0	0^{++}	0^{--}	1.0977	0.523
	$\Upsilon^h(3^3S_1)$	0	1	1	1^{+-}	1^{-+}	1.1027	0.4655
4 S	$\eta_b^h(4^1S_0)$	0	0	0	0^{++}	0^{--}	1.3000	0.6062
	$\Upsilon^h(4^3S_1)$	0	1	1	1^{+-}	1^{-+}	1.3039	0.5525
5 S	$\eta_b^h(5^1S_0)$	0	0	0	0^{++}	0^{--}	1.4864	0.6584
	$\Upsilon^h(5^3S_1)$	0	1	1	1^{+-}	1^{-+}	1.4895	0.6112
6 S	$\eta_b^h(6^1S_0)$	0	0	0	0^{++}	0^{--}	1.6606	0.6932
	$\Upsilon^h(6^3S_1)$	0	1	1	1^{+-}	1^{-+}	1.6632	0.6524
1P	$h_b^h(1^1P_1)$	1	0	1	1^{--}	1^{++}	0.7601	≈ 0
	$\chi_0^h(1^3P_0)$	1	1	0	0^{-+}	0^{+-}	0.7564	≈ 0
	$\chi_1^h(1^3P_1)$	1	1	1	1^{-+}	1^{+-}	0.7594	≈ 0
	$\chi_2^h(1^3P_2)$	1	1	2	2^{-+}	2^{+-}	0.7623	≈ 0
2 P	$h_b^h(2^1P_1)$	1	0	1	1^{--}	1^{++}	1.0014	≈ 0
	$\chi_0^h(2^3P_0)$	1	1	0	0^{-+}	0^{+-}	0.9996	≈ 0
	$\chi_1^h(2^3P_1)$	1	1	1	1^{-+}	1^{+-}	1.0015	≈ 0
	$\chi_2^h(2^3P_2)$	1	1	2	2^{-+}	2^{+-}	1.0035	≈ 0
3 P	$h_b^h(3^1P_1)$	1	0	1	1^{--}	1^{++}	1.2126	≈ 0
	$\chi_0^h(3^3P_0)$	1	1	0	0^{-+}	0^{+-}	1.2115	≈ 0
	$\chi_1^h(3^3P_1)$	1	1	1	1^{-+}	1^{+-}	1.2131	≈ 0
	$\chi_2^h(3^3P_2)$	1	1	2	2^{-+}	2^{+-}	1.2149	≈ 0
4 P	$h_b^h(4^1P_1)$	1	0	1	1^{--}	1^{++}	1.4048	≈ 0
	$\chi_0^h(4^3P_0)$	1	1	0	0^{-+}	0^{+-}	1.4041	≈ 0
	$\chi_1^h(4^3P_1)$	1	1	1	1^{-+}	1^{+-}	1.4054	≈ 0
	$\chi_2^h(4^3P_2)$	1	1	2	2^{-+}	2^{+-}	1.4071	≈ 0
5 P	$h_b^h(5^1P_1)$	1	0	1	1^{--}	1^{++}	1.5834	≈ 0
	$\chi_0^h(5^3P_0)$	1	1	0	0^{-+}	0^{+-}	1.5829	≈ 0
	$\chi_1^h(5^3P_1)$	1	1	1	1^{-+}	1^{+-}	1.5841	≈ 0
	$\chi_2^h(5^3P_2)$	1	1	2	2^{-+}	2^{+-}	1.5858	≈ 0
6 P	$h_b^h(6^1P_1)$	1	0	1	1^{--}	1^{++}	1.7514	≈ 0
	$\chi_0^h(6^3P_0)$	1	1	0	0^{-+}	0^{+-}	1.7512	≈ 0
	$\chi_1^h(6^3P_1)$	1	1	1	1^{-+}	1^{+-}	1.7521	≈ 0
	$\chi_2^h(6^3P_2)$	1	1	2	2^{-+}	2^{+-}	1.7538	≈ 0
1 D	$\eta_{b2}^h(1^1D_2)$	2	0	2	2^{++}	2^{--}	0.8771	≈ 0
	$\Upsilon^h(1^3D_1)$	2	1	1	1^{+-}	1^{-+}	0.8726	≈ 0
	$\Upsilon_2^h(1^3D_2)$	2	1	2	2^{+-}	2^{-+}	0.8761	≈ 0
	$\Upsilon_3^h(1^3D_3)$	2	1	3	3^{+-}	3^{-+}	0.8799	≈ 0
2 D	$\eta_{b2}^h(2^1D_2)$	2	0	2	2^{++}	2^{--}	1.1058	≈ 0
	$\Upsilon^h(2^3D_1)$	2	1	1	1^{+-}	1^{-+}	1.1025	≈ 0
	$\Upsilon_2^h(2^3D_2)$	2	1	2	2^{+-}	2^{-+}	1.1051	≈ 0
	$\Upsilon_3^h(2^3D_3)$	2	1	3	3^{+-}	3^{-+}	1.1080	≈ 0

n	Meson	L	S	J	J^{PC}		our calculated $\sqrt{\langle r^2 \rangle}$	our calculated $ R(0) ^2$
					$\varepsilon = 1$	$\varepsilon = -1$		
							fm	GeV^3
3 D	$\eta_{b2}^h(3^1D_2)$	2	0	2	2^{++}	2^{--}	1.3087	≈ 0
	$\Upsilon^h(3^3D_1)$	2	1	1	1^{+-}	1^{-+}	1.3059	≈ 0
	$\Upsilon_2^h(3^3D_2)$	2	1	2	2^{+-}	2^{-+}	1.3081	≈ 0
	$\Upsilon_3^h(3^3D_3)$	2	1	3	3^{+-}	3^{-+}	1.3108	≈ 0
4 D	$\eta_{b2}^h(4^1D_2)$	2	0	2	2^{++}	2^{--}	1.4947	≈ 0
	$\Upsilon^h(4^3D_1)$	2	1	1	1^{+-}	1^{-+}	1.4922	≈ 0
	$\Upsilon_2^h(4^3D_2)$	2	1	2	2^{+-}	2^{-+}	1.4943	≈ 0
	$\Upsilon_3^h(4^3D_3)$	2	1	3	3^{+-}	3^{-+}	1.4969	≈ 0
5 D	$\eta_{b2}^h(5^1D_2)$	2	0	2	2^{++}	2^{--}	1.6685	≈ 0
	$\Upsilon^h(5^3D_1)$	2	1	1	1^{+-}	1^{-+}	1.6661	≈ 0
	$\Upsilon_2^h(5^3D_2)$	2	1	2	2^{+-}	2^{-+}	1.6682	≈ 0
	$\Upsilon_3^h(5^3D_3)$	2	1	3	3^{+-}	3^{-+}	1.6707	≈ 0
1 F	$h_{b3}^h(1^1F_3)$	3	0	3	3^{--}	3^{++}	0.9856	≈ 0
	$\chi_2^h(1^3F_2)$	3	1	2	2^{-+}	2^{+-}	0.9806	≈ 0
	$\chi_3^h(1^3F_3)$	3	1	3	3^{-+}	3^{+-}	0.9847	≈ 0
	$\chi_4^h(1^3F_4)$	3	1	4	4^{-+}	4^{+-}	0.9891	≈ 0
2 F	$h_{b3}^h(2^1F_3)$	3	0	3	3^{--}	3^{++}	1.2029	≈ 0
	$\chi_2^h(2^3F_2)$	3	1	2	2^{-+}	2^{+-}	1.1989	≈ 0
	$\chi_3^h(2^3F_3)$	3	1	3	3^{-+}	3^{+-}	1.2023	≈ 0
	$\chi_4^h(2^3F_4)$	3	1	4	4^{-+}	4^{+-}	1.206	≈ 0
3 F	$h_{b3}^h(3^1F_3)$	3	0	3	3^{--}	3^{++}	1.3983	≈ 0
	$\chi_2^h(3^3F_2)$	3	1	2	2^{-+}	2^{+-}	1.3947	≈ 0
	$\chi_3^h(3^3F_3)$	3	1	3	3^{-+}	3^{+-}	1.3977	≈ 0
	$\chi_4^h(3^3F_4)$	3	1	4	4^{-+}	4^{+-}	1.4012	≈ 0
4 F	$h_{b3}^h(4^1F_3)$	3	0	3	3^{--}	3^{++}	1.5777	≈ 0
	$\chi_2^h(4^3F_2)$	3	1	2	2^{-+}	2^{+-}	1.5759	≈ 0
	$\chi_3^h(4^3F_3)$	3	1	3	3^{-+}	3^{+-}	1.5785	≈ 0
	$\chi_4^h(4^3F_4)$	3	1	4	4^{-+}	4^{+-}	1.5817	≈ 0

Table 7: $S \rightarrow P$, E1 radiative transitions. Experimental results are taken from Ref. [36]. The masses are taken from above mentioned Table 1 and 2; we use the experimental masses if known. Otherwise, theoretically calculated masses are used.

Transition	Initial Meson	Final Meson	Our calculated Γ_{E1}		Exp.[36] Γ_{E1}	Our calculated Γ_{E1} for Hybrid	
			NR	Relativistic		NR	Relativistic
			keV	keV	keV	keV	keV
$2S \rightarrow 1P$	$\Upsilon(2^3S_1)$	$\chi_2(1^3P_2)$	2.92446	3.1721	2.29 ± 0.23	5.1971	1.1754
		$\chi_1(1^3P_1)$	2.8324	3.0722	2.21 ± 0.22	3.2521	0.7353
		$\chi_0(1^3P_0)$	1.8530	2.0099	1.22 ± 0.16	1.197	0.2713
		$\eta_b(2^1S_0)$	4.5379	6.1059	-	8.9043	2.0837
$3S \rightarrow 2P$	$\Upsilon(3^3S_1)$	$\chi_2(2^3P_2)$	3.5085	3.9429	2.66 ± 0.41	9.8022	1.8071
		$\chi_1(2^3P_1)$	3.2114	3.60897	2.56 ± 0.34	6.0429	1.9948
		$\chi_0(2^3P_0)$	1.9819	2.2273	1.2 ± 0.16	2.1899	0.4837
		$\eta_b(3^1S_0)$	3.3529	1.0037	-	16.3702	3.2650
$3S \rightarrow 1P$	$\Upsilon(3^3S_1)$	$\chi_2(1^3P_2)$	0.478	0.8894	-	0.2822	0.0001752
		$\chi_1(1^3P_1)$	0.3247	0.6041	-	0.1719	0.0001779
		$\chi_0(1^3P_0)$	0.1323	0.2461	-	0.0594	0.00003697
		$\eta_b(3^1S_0)$	0.7162	1.0104	-	0.5856	0.003845
$4S \rightarrow 3P$	$\Upsilon(4^3S_1)$	$\chi_2(3^3P_2)$	16.1868	22.1972	-	13.5065	2.1898
		$\chi_1(3^3P_1)$	9.8560	17.0252	-	8.2744	1.5411
		$\chi_0(3^3P_0)$	3.4652	7.7808	-	2.9573	0.6656
		$\eta_b(4^1S_0)$	4.6883	1.5278	-	22.4101	4.1018
$4S \rightarrow 2P$	$\Upsilon(4^3S_1)$	$\chi_2(2^3P_2)$	0.2995	0.5918	-	0.4292	0.002269
		$\chi_1(2^3P_1)$	0.2029	0.401	-	0.25998	0.002348
		$\chi_0(2^3P_0)$	0.0826	0.1632	-	0.0892	0.000503
		$\eta_b(4^1S_0)$	0.5538	0.5644	-	0.8547	0.0150
$4S \rightarrow 1P$	$\Upsilon(4^3S_1)$	$\chi_2(^3P_2)$	0.2212	0.3857	-	0.1655	0.006019
		$\chi_1(^3P_1)$	0.144	0.251	-	0.1002	0.006076
		$\chi_0(^3P_0)$	0.0549	0.0957	-	0.0341	0.001244
		$\eta_b(4^1S_0)$	0.361	0.4644	-	0.3235	0.01693

Table 8: 1P and 2P, E1 radiative transitions.

Transition	Initial Meson	Final Meson	Our calculated Γ_{E1}		Our calculated Γ_{E1} for Hybrid	
			NR	Relativistic	NR	Relativistic
			keV	keV	keV	keV
$1P \rightarrow 1S$	$\chi_2(1^3P_2)$	$\Upsilon(1^3S_1)$	37.2672	32.4094	0.1059	0.5231
	$\chi_1(1^3P_1)$		32.8195	14.0823	0.0999	0.4918
	$\chi_0(1^3P_0)$		26.0114	11.1611	0.0863	0.4192
	$h_b(1^1P_1)$		22.8589	23.0341	0.100875	0.5217
$2P \rightarrow 2S$	$\chi_2(2^3P_2)$	$\Upsilon_2(2^3S_1)$	18.9917	17.9986	0.433731	1.2147
	$\chi_1(2^3P_1)$		16.1418	15.2977	0.4206	1.0871
	$\chi_0(2^3P_0)$		11.8767	11.2557	0.3813	0.8543
	$h_b(2^1P_1)$		12.793	13.065	0.4483	1.1985
$2P \rightarrow 1S$	$\chi_2(2^3P_2)$	$\Upsilon(1^3S_1)$	14.3444	16.5078	0.3136	0.0803
	$\chi_1(2^3P_1)$		13.6951	7.7764	0.3106	0.0775
	$\chi_0(2^3P_0)$		12.6092	7.1582	0.3013	0.072
	$h_b(2^1P_1)$		10.4703	12.9422	0.3277	0.0641
$2P \rightarrow 1D$	$\chi_2(2^3P_2)$	$\Upsilon_3(1^3D_3)$	2.8853	2.1582	1.4575	1.2894
		$\Upsilon_2(1^3D_2)$	1.0543	0.5806	0.2706	0.2312
		$\Upsilon(1^3D_1)$	0.07872	0.0493	0.01934	0.0158
	$\chi_1(2^3P_1)$	$\Upsilon_2(1^3D_2)$	3.8710	1.9464	1.3200	1.0596
		$\Upsilon(1^3D_1)$	1.4630	0.8546	0.4720	0.3637
	$\chi_0(2^3P_0)$	$\Upsilon(1^3D_1)$	3.2108	1.5811	1.7476	1.2093
	$h_b(2^1P_1)$	$\eta_{2b}(1^1D_2)$	1.9096	1.0775	1.7699	1.4554

- [32] K.A. Olive et al. (Particle Data Group), Chin. Phys. C **38**, 090001 (2014) and (2015) update.
- [33] Jorge Segovia, David R. Entem, Francisco Fernandez, Phys. Rev. D **91**, 014002 (2015).
- [34] Wei Chen, R. T. Kleiv, T. G. Steele, B. Bulthuis, D. Harnett, J. Ho, T.Richards, Shi-Lin Zhu, JHEP, **1309** , 019, (2013).
- [35] Bai-Qing Li, Kuang-Ta Chao, Commun. Theor. Phys. **52**, 653,(2009).
- [36] J. Beringer et al. (Particle Data Group), PR D**86**, 010001 (2012).
- [37] J. Ferretti, EPJ Web of conferences **96**, 01012, (2015).

Table 9: 3P E1 radiative transitions..

Transition	Initial Meson	Final Meson	Our calculated Γ_{E1}		Others Theo. calculated Γ_{E1} [37]	Our calculated Γ_{E1} for Hybrid	
			NR	Relativistic		NR	Relativistic
			keV	keV	keV	keV	keV
$3P \rightarrow 3S$	$\chi_2(3^3P_2)$	$\Upsilon(3^3S_1)$	2.7868	2.1708	8.2	0.9052	1.9761
	$\chi_1(3^3P_1)$		2.7389	1.5024	7.4	0.8862	1.6942
	$\chi_0(3^3P_0)$		2.568	0.8133	6.1	0.8238	1.2692
	$h_b(3^1P_1)$	$\eta_b(3^1S_0)$	43.5866	10.5692	-	3.8295	1.9078
$3P \rightarrow 2S$	$\chi_2(3^3P_2)$	$\Upsilon(2^3S_1)$	3.8179	4.4072	3.8	0.4942	0.02428
	$\chi_1(3^3P_1)$		3.8027	4.0832	2.5	0.4909	0.0231
	$\chi_0(3^3P_0)$		3.7472	3.6518	1.2	0.4795	0.02107
	$h_b(3^1P_1)$	$\eta_b(2^1S_0)$	4.3418	4.45835	-	0.5146	0.01186
$3P \rightarrow 1S$	$\chi_2(3^3P_2)$	$\Upsilon(1^3S_1)$	6.5022	4.087	3.9	0.3655	0.0182
	$\chi_1(3^3P_1)$		6.4914	3.9609	2.1	0.3640	0.01762
	$\chi_0(3^3P_0)$		6.4517	3.7867	0.6	0.3591	0.01670
	$h_b(3^1P_1)$	$\eta_b(1^1S_0)$	6.05386	7.4577	-	0.3936	0.01225
$3P \rightarrow 2D$	$\chi_2(3^3P_2)$	$\Upsilon_3(2^3D_3)$	2.7611	1.7238	-	2.7122	2.2670
		$\Upsilon_2(2^3D_2)$	0.5294	0.4278	-	0.5011	0.41735
		$\Upsilon(2^3D_1)$	0.03922	0.0422	0	0.03547	0.02942
		$\Upsilon_2(2^3D_2)$	2.5888	1.2959	-	2.4588	1.8188
	$\chi_1(3^3P_1)$	$\Upsilon(2^3D_1)$	0.959694	0.02735	0.4	0.8704	0.6427
		$\Upsilon(2^3D_1)$	3.5427	1.2941	0.9	3.2659	2.0013
		$\Upsilon_{2b}(2^1D_2)$	3.2641	1.8727	-	3.2554	2.5194
		$\Upsilon_{2b}(2^1D_2)$	3.2641	1.8727	-	3.2554	2.5194
$3P \rightarrow 1D$	$\chi_2(3^3P_2)$	$\Upsilon_3(1^3D_3)$	0.003086	0.00995	-	0.00151096	0.009085
		$\Upsilon_2(1^3D_2)$	0.0007225	0.002046	-	0.0002736	0.001625
		$\Upsilon(1^3D_1)$	0.00005047	0.0001492	0	0.00001871	0.0001094
		$\Upsilon_2(1^3D_2)$	0.003593	0.009114	0	0.001359	0.0077515
	$\chi_1(3^3P_1)$	$\Upsilon(1^3D_1)$	0.001255	0.0001334	0	0.0004648	0.002611
		$\Upsilon(1^3D_1)$	0.004922	0.01129	0.2	0.001819	0.009612
		$\Upsilon_{2b}(1^1D_2)$	0.011687	0.01829	-	0.004486	0.009124
		$\Upsilon_{2b}(1^1D_2)$	0.011687	0.01829	-	0.004486	0.009124

Table 10: 1D and 2D, E1 radiative transitions.

Transition	Initial Meson	Final Meson	Our calculated Γ_{E1}		Our calculated Γ_{E1} for Hybrid	
			NR	Relativistic	NR	Relativistic
			keV	keV	keV	keV
$1D \rightarrow 1P$	$\Upsilon_3(1^3D_3)$	$\chi_2(1^3P_2)$	31.2721	37.4118	0.697128	1.3347
	$\Upsilon_2(1^3D_2)$	$\chi_2(1^3P_2)$	5.48044	8.0209	0.166202	0.3319
		$\chi_1(1^3P_1)$	21.025	29.9376	0.525086	1.0501
	$\Upsilon(1^3D_1)$	$\chi_2(1^3P_2)$	0.568022	0.8016	0.016906	0.0355
		$\chi_1(1^3P_1)$	10.9584	15.0785	0.267473	0.5621
		$\chi_0(1^3P_0)$	21.5026	28.5597	0.404108	0.8539
	$h_{b2}(1^1D_2)$	$h_c(1^1P_1)$	25.8402	37.5565	0.683847	1.3757
$2D \rightarrow 2P$	$\Upsilon_3(2^3D_3)$	$\chi_2(2^3P_2)$	5.066356	6.26455	1.243	1.8549
	$\Upsilon_2(2^3D_2)$	$\chi_2(2^3P_2)$	1.20268	1.2878	0.298876	0.4466
		$\chi_1(2^3P_1)$	5.06132	5.4054	0.924251	1.4978
	$\Upsilon(2^3D_1)$	$\chi_2(2^3P_2)$	0.123364	0.1075	0.0309465	0.04621
		$\chi_1(2^3P_1)$	2.61871	2.3302	0.478846	0.07770
		$\chi_0(2^3P_0)$	5.87955	5.3734	0.702497	1.2922
	$\eta_{b2}(2^1D_2)$	$h_c(2^1P_1)$	13.7231	11.658	1.2211	1.9484
$2D \rightarrow 1P$	$\Upsilon_3(2^3D_3)$	$\chi_2(1^3P_2)$	2.90251	3.9918	0.3328	0.0460
	$\Upsilon_2(2^3D_2)$	$\chi_2(1^3P_2)$	0.717137	0.9530	0.0822195	0.01137
		$\chi_1(1^3P_1)$	2.42052	3.2158	0.250619	0.0347
	$\Upsilon(2^3D_1)$	$\chi_2(1^3P_2)$	0.0782558	0.09939	0.00894224	0.001238
		$\chi_1(1^3P_1)$	1.32166	1.6815	0.136303	0.01887
		$\chi_0(1^3P_0)$	2.13601	2.7245	0.188855	0.02628
	$h_{b2}(2^1D_2)$	$h_c(1^1P_1)$	3.31247	4.3669	0.354383	0.04394
$2D \rightarrow 1F$	$\Upsilon_3(2^3D_3)$	$\chi_4(1^3F_4)$	1.5356	1.1737	1.37234	1.1421
		$\chi_3(1^3F_3)$		0.1113		0.09658
		$\chi_2(1^3F_2)$		0.003629		0.002759
	$\Upsilon_2(2^3D_2)$	$\chi_3(1^3F_3)$	1.56236	0.9104	0.31346	0.9903
		$\chi_2(1^3F_2)$		0.13177		0.1311
	$\Upsilon(2^3D_1)$	$\chi_2(1^3F_2)$		0.7497		1.1141
	$\eta_{b2}(2^1D_2)$	$h_{c3}(1^1F_3)$	1.73254	1.0752	1.48814	1.19693

Table 11: 1F E1 radiative transitions.

Transition	Initial Meson	Final Meson	Our calculated Γ_{E1}		Our calculated Γ_{E1} for Hybrid	
			NR	Relativistic	NR	Relativistic
			keV	keV	keV	keV
$1F \rightarrow 1D$	$\chi_4(1^3F_4)$	$\Upsilon_3(1^3D_3)$	9.5648	10.9949	1.59592	2.2932
	$\chi_3(1^3F_3)$	$\Upsilon_3(1^3D_3)$	0.986547	1.1616	0.173011	0.2612
		$\Upsilon_2(1^3D_2)$	14.2317	12.348	1.44778	2.1002
	$\chi_2(1^3F_2)$	$\Upsilon_3(1^3D_3)$	0.0357111	0.0430	0.00655625	0.0104
		$\Upsilon_2(1^3D_2)$	2.2958	2.01672	0.240224	0.3675
		$\Upsilon(1^3D_1)$	13.676	13.004	1.40738	2.0543
	$h_{b3}(1^1F_3)$	$\eta_{c2}(1^1D_2)$	15.9777	13.2407	1.6188	2.3504

Table 12: 2F E1 radiative transitions

Transition	Initial Meson	Final Meson	Our calculated Γ_{E1}		Our calculated Γ_{E1} for Hybrid	
			NR	Relativistic	NR	Relativistic
			keV	keV	keV	keV
$2F \rightarrow 2D$	$\chi_4(2^3F_4)$	$\Upsilon_3(2^3D_3)$	14.0995	10.4506	2.21899	2.7635
	$\chi_3(2^3F_3)$	$\Upsilon_3(2^3D_3)$	1.50403	1.07438	0.239362	0.3086
		$\Upsilon_2(2^3D_2)$	12.561	10.3987	1.98909	2.559
	$\chi_2(2^3F_2)$	$\Upsilon_3(2^3D_3)$	0.0565314	0.03851	0.00909425	0.01215
		$\Upsilon_2(2^3D_2)$	2.06744	1.6423	0.33085	0.4410
		$\Upsilon(2^3D_1)$	11.9235	11.3486	1.91142	2.5432
	$h_{b3}(2^1F_3)$	$\eta_{c2}(2^1D_2)$	14.1418	11.3816	2.22003	2.8476
$2F \rightarrow 1D$	$\chi_4(2^3F_4)$	$\Upsilon_3(1^3D_3)$	1.05143	1.1283	0.288102	0.01506
	$\chi_3(2^3F_3)$	$\Upsilon_3(1^3D_3)$	0.115071	0.1220	0.0317167	0.001676
		$\Upsilon_2(1^3D_2)$	1.15993	1.1003	0.257443	0.01343
	$\chi_2(2^3F_2)$	$\Upsilon_3(1^3D_3)$	0.00449888	0.004701	0.00124863	0.00006671
		$\Upsilon_2(1^3D_2)$	0.198759	0.1858	0.0443444	0.002339
		$\Upsilon(1^3D_1)$	1.11751	1.0837	0.245853	0.01277
	$h_{b3}(2^1F_3)$	$\eta_{c2}(1^1D_2)$	1.32504	1.2458	0.294385	0.01485

Table 13: M1 radiative transitions.

Transition	Initial Meson	Final Meson	Our calculated Γ_{M1}		Our calculated Γ_{M1} for Hybrid	
			NR	Relativistic	NR	Relativistic
			keV	keV	keV	keV
1S	$J/\Upsilon(1^3S_1)$	$\eta_c(1^1S_0)$	0.000492035	0.0002302	1.01944×10^{-7}	4.5204×10^{-8}
2S	$\Upsilon(2^3S_1)$	$\dot{\eta}_c(2^1S_0)$	0.000324864	0.00004591	6.4119×10^{-7}	2.6351×10^{-7}
		$\eta_c(1^1S_0)$	0.00276436	0.0008832	0.0000715969	9.3836×10^{-6}
	$\dot{\eta}_c(2^1S_0)$		0.00669986	0.003021	0.000204514	0.00002694
3S	$\Upsilon(3^3S_1)$	$\eta_c(3^1S_0)$	0.0119813	0.01948	1.01831×10^{-6}	4.1833×10^{-7}
		$\dot{\eta}_c(2^1S_0)$	0.000484597	0.000151	0.0000379935	0.00001922
		$\eta_c(1^1S_0)$	0.00263485	0.0007183	0.000125394	0.0000196
	$\eta_c(3^1S_0)$	$\Upsilon(2^3S_1)$	0.000694522	0.0001993	0.00010799	0.00005409
		$J/\Upsilon(1^3S_1)$	0.005646	0.001816	0.000348385	0.00005519
2 P	$\dot{h}_c(2^1P_1)$	$\chi_2(1^3P_2)$	0.000146288	0.0001772	0.0000182371	3.6028×10^{-7}
		$\chi_1(1^3P_1)$	0.000104884	0.0001261	0.0000111999	2.2125×10^{-7}
		$\chi_0(1^3P_0)$	0.000046339	0.00005515	3.9463×10^{-6}	7.8111×10^{-8}
	$\dot{\chi}_2(2^3P_2)$	$h_c(1^1P_1)$	0.000145937	0.0001566	0.0000111183	2.26827×10^{-7}
	$\dot{\chi}_1(2^3P_1)$	$h_c(1^1P_1)$	0.000131292	0.0001409	0.0000109691	2.1607×10^{-7}
	$\dot{\chi}_0(2^3P_0)$	$h_c(1^1P_1)$	0.000108136	0.000116	0.0000105088	1.9511×10^{-7}